

## $^{144}\text{Ce}$ — $^{144}\text{Pr}$ electron antineutrino spectrum measurement with silicon semiconductor detectors

© A.V. Derbin, I.S. Drachnev, I.M. Kotina, V.N. Muratova, N.V. Niyazova, D.A. Semenov,  
M.V. Trushin, E.V. Unzhakov

St. Petersburg Nuclear Physics Institute, National Research Center Kurchatov Institute, Gatchina, Russia  
E-mail: niyazova\_nv@pnpi.nrcki.ru

Received May 12, 2023

Revised May 12, 2023

Accepted October, 30, 2023

In this work we present  $\beta$ -spectrum studies for  $^{144}\text{Ce}$ — $^{144}\text{Pr}$  source spectra with endpoint energy of 2997 keV. The spectral studies were performed with two spectrometer types: target–detector scheme and a  $4\pi$  spectrometer. The spectra were fitted with the spectrometer response functions derived through Monte-Carlo simulations. As a result of the study, we have derived the nuclear shape factor necessary for the  $\beta$ -spectrum calculation. The obtained parameters of the shape factor agree between the spectrometers within statistical uncertainties. Also, we have evaluated electron antineutrino spectrum of  $^{144}\text{Pr}$  decay with the most precise up to date rate expected for IBD on protons of  $(0.47091 \pm 0.00003_{\text{stat}} + 0.00022_{\text{sys}}) \cdot 10^{-43} \text{ cm}^2 \text{ decay}^{-1}$ .

**Keywords:**  $\beta$ -decay, beta-decay,  $^{144}\text{Ce}$ — $^{144}\text{Pr}$ , neutrino.

DOI: 10.61011/TPL.2023.12.57589.65A

The artificial source of electron antineutrinos  $^{144}\text{Ce}$ — $^{144}\text{Pr}$  is one of the most promising for experiments to search for neutrino oscillations to the sterile state at short distances. This source was planned to be used in the Borexino SOX [1] and CeLAND [2], experiments, but the experiments were not carried out for reasons other than technical problems. The  $^{144}\text{Ce}$ — $^{144}\text{Pr}$  source remains the most attractive source for future experiments, and accurate knowledge of the shape of  $\beta$ -spectra of  $^{144}\text{Ce}$ — $^{144}\text{Pr}$  is a prerequisite for achieving high sensitivity to oscillation parameters. In the present work, silicon semiconductor detectors were used to measure  $\beta$ -spectra. In addition to the classical  $\beta$  spectrometer target–detector scheme, we have developed an  $4\pi$  spectrometer consisting of two detectors. Precision modelling of the plant geometry allowed reliable reproduction of the response functions of the spectrometers used.

The first spectrometer, based on a target–detector scheme, consisted of a semiconductor Si(Li)-detector with a thickness of 10.2 mm and a sensing area diameter of 20 mm (Fig. 1, *a*). The thickness of the insensitive diffuse lithium layer at the back of the detector was 0.42 mm [3,4]. A detector with such parameters provided complete absorption of  $\beta$ -disintegration  $^{144}\text{Ce}$ — $^{144}\text{Pr}$  electrons with energies up to 3 MeV. The detector was mounted in a mandrel with a tungsten collimator with a diameter of 12 mm. The  $^{144}\text{Ce}$  source was applied to a 50  $\mu\text{m}$  thick lavalan substrate,  $\mu\text{m}$  in the form of a dried drop of colloidal solution, and then the substrate was placed over the detector surface at a distance of 8.9 mm. The whole structure was placed in a vacuum cryostat and cooled to liquid nitrogen temperature. The energy calibration of the spectrometer was carried out using an  $^{207}\text{Bi}$  source. The small impurity  $\alpha$ -activity of  $^{241}\text{Am}$ - and  $^{244}\text{Cm}$ -sources was used to find the target thickness distribution, which averaged 1  $\mu\text{m}$ . Additionally, a

scintillation BGO detector with a mass of 2.5 kg was added to the setup to allow time-amplitude coincidence analysis to extract the spectrum of the resolved  $^{144}\text{Pr}(0^-) \rightarrow ^{144}\text{Nd}(1^-)$  transition.

The second spectrometer consisted of two Si(Li)-detectors with a sensitive region thickness greater than 8.5 mm, which also exceeds the path length of electrons with energy 3 MeV (Fig. 1, *b*). The diameters of the sensitive area of the detectors were 20 and 18 mm. Both detectors were characterized and calibrated using an  $^{207}\text{Bi}$  source. The energy resolution of the detectors was 2 keV. The thickness of the insensitive detector region, consisting of a sputtered palladium and gold layer and a silicon surface layer, was 500 nm silicon equivalent, with the back side of the diffuse lithium contact 0.4 mm [4]. A well with a diameter of 5 mm and a depth of 1 mm was ground in one of the detectors, where the  $^{144}\text{Ce}$ — $^{144}\text{Pr}$  source was applied in the form of a dried drop. A second detector was superimposed on top without any gap, and a bias voltage was applied to the common  $n^+$ -pin.

The spectrometers were equipped with charge-sensitive preamplifiers with field-effect transistors, which were placed next to the detectors inside a cryostat and cooled to the temperature of liquid nitrogen. The signals were fed to a CAEN v1725 digitizer and digitized at a sampling rate of 250 MHz.

On the first type of unit, 2024 clock series were accumulated and sampled and divided into two equal parts. The difference between the first and second parts of the data allowed to significantly reduce the contribution of background disintegrations, which constituted a significant part of the measured spectrum due to the large age of the source  $^{144}\text{Ce}$ — $^{144}\text{Pr}$ . The spectrum of the first part was fitted by the sum of the spectrum for the second part,  $\beta$ - $^{144}\text{Ce}$  and  $^{144}\text{Pr}$  spectra and background components.

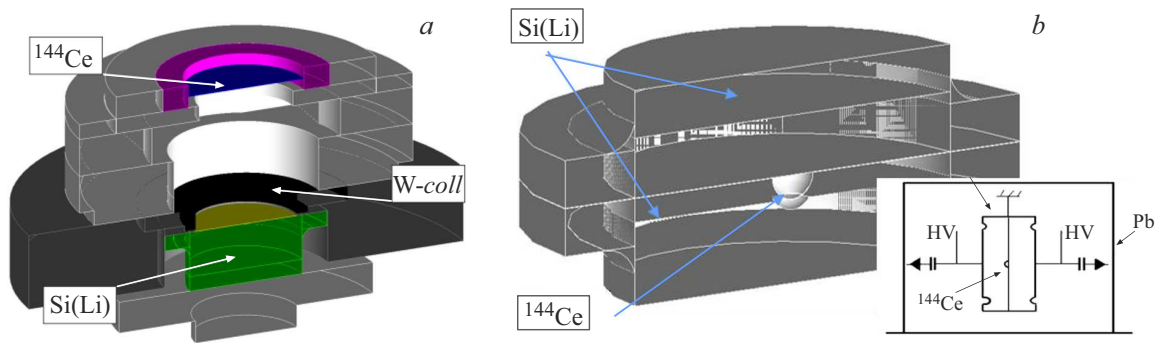


**Figure 1.** *a* — schematic image of the spectrometer in detector target geometry; *b* — schematic image of the spectrometer in  $4\pi$  geometry.

The  $\beta$ -spectrum is described as follows:

$$S(W) = F(Z, W)C(W)PW(W - W_0)^2,$$

where  $P$  and  $T$  — the momentum and kinetic energy of the electron,  $W = T/mc^2 + 1$  — the total energy of the electron,  $F(Z, W)$  — the Fermi function describing the electromagnetic interaction of the electron with atom. Various corrections to the Fermi function have been taken into account, among which radiation corrections, size finiteness corrections, and corrections for weak magnetism are major contributors. The nuclear form factor  $C(W)$  is the sought function to determine the shape of the  $\beta$ -spectrum of the forbidden transition. The form factor was parameterized as

$$C(W) = 1 + C_1W + C_2W^{-1},$$

where  $C_1$  and  $C_2$  — free parameters.

The measured spectrum is a convolution of the theoretical  $\beta$ -spectrum and the  $R(E, W)$  detector response function to an electron with energy  $W$  ( $E$  — the recorded energy). The detector function was modelled using the Monte Carlo method (GEANT4.10.6 package). The simulation fully reproduced the geometry of the facility, taking into account the thicknesses of the insensitive detector layers and the target thickness distribution. The main background component was related to the activity of the isotope  $^{154}\text{Eu}$ , whose spectrum was also simulated by Monte Carlo simulation.

The measured spectrum was fitted by the maximum likelihood method with using the  $\chi^2$  function (Fig. 2). The following expression for the formfactor function was derived for the setting in the detector target circuit:

$$C(W) = 1 + (-0.023 \pm 0.005)W + (-0.17 \pm 0.09)W^{-1}. \quad (1)$$

In addition to this, a fitting of the resolved transition spectrum was performed, which showed good agreement between the model and experiment. The accuracy of the  $C_1$  and  $C_2$  parameters is limited by the low source activity and the uncertainty in the detector response function associated with electron backscattering from the crystal surface.

The advantage of the spectrometer with  $4\pi$ -geometry is that the response function for each electron energy is close to the  $\delta$ -function, since the chosen geometry allows the energy of the reflected electrons to be measured. The difference of the response function from the Gaussian one is due to the passage of electrons through the insensitive region of the detector, which was taken into account by introducing an additional exponential „tail“, the intensity and shape of which depended on two additional parameters. The following values of the parameters of the form factor function are obtained as a result of the fitting:

$$C(W) = 1 + (-0.0288 \pm 0.0003)W + (-0.117 \pm 0.003)W^{-1}. \quad (2)$$

When comparing the results obtained (1) and (2), it can be seen that they agree with each other within the limits of error. Moreover, the found values of  $C_1$  and  $C_2$  agree with the results obtained in [5–7] but with better accuracy.

The neutrino spectrum is calculated from the measured  $\beta$ -spectrum, taking into account the conservation of energy in the disintegration process. For oscillation experiments, it is important to know the shape and part of the neutrino spectrum above the threshold of the  $\beta$ -disintegration back reaction on hydrogen 1.8 MeV. The main contribution to the spectrum above the threshold is made by neutrinos from the two most probable disintegration modes of  $^{144}\text{Pr}$ : the transition to the ground state of the  $^{144}\text{Nd}$  nucleus with a probability of 97.9% and a boundary energy of  $Q = 2997.5$  keV and a unique forbidden transition of the first kind to the  $2^+$  level of the  $^{144}\text{Nd}$  nucleus (1.04%,  $Q = 2301$  keV). The fraction of the neutrino spectrum with energies above 1.8 MeV is  $0.50467 \pm 0.00003$ . Considering the dependence of the backward  $\beta$ -disintegration cross section on the neutrino energy, we can estimate the reduced effective cross section for the source  $^{144}\text{Pr}$ , which was  $(0.47091 \pm 0.00003_{stat} + 0.00022_{sys}) \cdot 10^{-43} \text{ cm}^2$  per one disintegration of the nucleus  $^{144}\text{Pr}$ . The accuracy of the obtained value (0.05%), due to the uncertainty in the shape of the neutrino spectrum, is an order of magnitude better than the accuracy of the determination of the

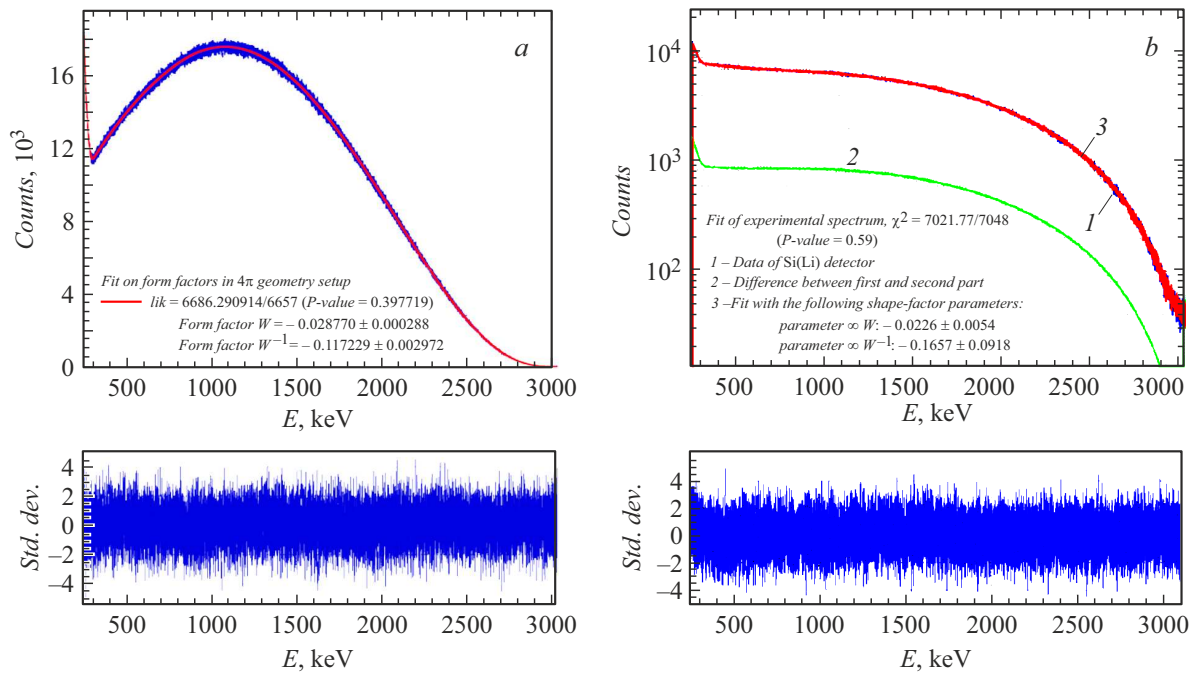


**Figure 2.** *a* —  $\beta$  spectrum of  $^{144}\text{Pr}$  measured by the spectrometer in  $4\pi$  geometry; *b* —  $\beta$  spectrum of  $^{144}\text{Pr}$  measured by the spectrometer in the detector target circuit (green indicates the spectrum of the difference of the two parts of the exposure). The difference between the fitting function and the measured spectra in units of standard deviation is presented at the bottom. A color version of the figure is provided in the online version of the paper.

$^{144}\text{Ce}$ – $^{144}\text{Pr}$  source activity using calorimetry (0.4%) in the Borexino SOX [8] experiment.

Thus in the present work, two types of spectrometers were used to measure and analyze the spectra of  $\beta$ -source  $^{144}\text{Ce}$ – $^{144}\text{Pr}$ . Parameter values for the nuclear transition form factor function  $^{144}\text{Pr}$  to the ground state  $^{144}\text{Nd}$  have been determined:

$$C(W) = 1 + (-0.0288 \pm 0.0003)W + (-0.117 \pm 0.003)W^{-1}.$$

The electron antineutrino spectrum was obtained and the reduced reaction cross section of the reverse  $\beta$ -disintegration for the  $^{144}\text{Ce}$ – $^{144}\text{Pr}$  source was calculated, which is  $(0.47091 \pm 0.00003_{\text{stat}} + 0.00022_{\text{sys}}) \cdot 10^{-43} \text{ cm}^2$  per one disintegration of the  $^{144}\text{Pr}$  nucleus.

## Funding

This study was supported by the Russian Science Foundation (project No. 21-12-00063).

## Conflict of interest

The authors declare that they have no conflict of interest.

## References

- [1] G. Bellini, D. Bick, G. Bonfini et al., *J. High Energy Phys.*, **2013**, 38 (2013). DOI: 10.1007/JHEP08(2013)038
- [2] A. Gando, Y. Gando, S. Hayashida et al., *arXiv:1312.0896* (2013). DOI: 10.48550/arXiv.1312.0896

- [3] S.V. Bakhlanov, A.V. Derbin, I.S. Drachnev, I.S. Lomskaya, I.M. Kotina, V.N. Muratova, N.V. Niyazova, M.V. Trushin, E.A. Chmel', *Phys. Atom. Nucl.*, **85** (6), 936 (2022). DOI: 10.1134/S1063778823010064
- [4] I.E. Alekseev, S.V. Bakhlanov, N.V. Bazlov, E.A. Chmel, A.V. Derbin, I.S. Drachnev, I.M. Kotina, M.S. Mikulich, V.N. Muratova, N.V. Niyazova, D.A. Semonov, M.V. Trushin, E.V. Unzhakov, *Nucl. Instrum. Meth. Phys. Res. A*, **1051**, 168242 (2023). DOI: 10.1016/j.nima.2023.168242
- [5] M.J. Laubitz, *Proc. Phys. Soc. A.*, **69** (11), 789 (1956). DOI: 10.1088/0370-1298/69/11/301
- [6] T. Nagarajan, M. Ravindranath, R.K. Venkata Reddy, *Nuovo Cimento A*, **3** (3), 699 (1971). DOI: 10.1007/BF02813571
- [7] H. Daniel, G.T. Kaschl, *Nucl. Phys.*, **76** (1), 97 (1966). DOI: 10.1016/0029-5582(66)90961-8
- [8] K. Altenmüller, M. Agostini, S. Appel et al., *Phys. Atom. Nucl.*, **79** (11-12), 1481 (2016). DOI: 10.1134/S106377881610001X

Translated by J.Deineka